Investigation of Reconstruction Algorithms by Means of Quantitative PET/CT Phantom Studies with a Focus on Evaluation Strategies

A PET/CT Phantom Study

Johannes Neuwirth[*1], Thomas Layer[2], Matthias Blaickner[3], Wolfgang Birkfellner[4], Anton Staudenherz[5]

[*1]Seibersdorf Laboratories – Radiation Safety and Applications, Seibersdorf, Austria

[2,3]Austrian Institute of Technologies, Health & Environment Department – Biomedical Systems, Vienna, Austria

[4]Center for Medical Physics and Biomedical Engineering AKH-MUW, Vienna, Austria

[5]Medical University of Vienna, Dept. of Biomedical Imaging and Image-Guided Therapy, Devision of Nuclear Medicine, AKH, Vienna, Austria

[*1]Johannes.neuwirth@seibersdorf-laboratories.at; [2]Thomas.Layer.fl@ait.ac.at; [3]Matthias.Blaickner@ait.ac.at; [4]wolfgang.birkfellner@meduniwien.ac.at; [5]anton.staudenherz@meduniwien.ac.at

***Abstract*-The aim of this work is to investigate the TrueX reconstruction algorithm and to compare different PET reconstruction algorithms (2D OSEM and 3D OSEM) using a phantom with non-spherical objects. Furthermore, different evaluation algorithms and their impact on activity analysis are explored. Measurements were carried out using a Siemens Biograph 64 TruePoint™ PET/CT Scanner and an in-house phantom. The measurements were carried out at four different signal to background ratios (SBR), using 18F-FDG. For evaluation purposes, three different algorithms were used: Adaptive Thresholding, Percentage Thresholding, and the Maximum Line Method. With regard to the two thresholding procedures, the effect of subtracting the voxels of the inactive plastic walls was investigated. TrueX produces rather large overestimates of the activity concentration of up to 25 % at diameters between 11 mm and 24 mm. The technique of stripping off the inactive hull after Adaptive and Percentage Thresholding considerably reduces the contribution of the partial volume effect, thus minimizing the underestimate, which is much more constant over the entire range of diameters. The thresholding procedures generate statistically stable results, but their detection efficiency decreases with decreasing diameter and SBR. The Maximum Line Method naturally yields results for all cylinders and parameter settings; however, this occurs at the cost of a higher relative uncertainty. For quantitative studies, such as quality assurance measurements with standard phantoms, 3D OSEM should be preferred.**

Keywords- TrueX; PET-CT; Activity Analysis; OSEM

I. BACKGROUND

Image quantification in clinical nuclear medicine is essential and crucially depends on the choice of the reconstruction algorithm [1]. Filtered back projection (FBP) has its limitations, especially when attenuation correction is incorporated [2], because it accentuates noise and produces streak artifacts that hamper quantification. Nearly 30 years ago, Iterative Reconstruction (IR) was introduced to improve Positron Emission Tomography (PET) image quality and quantification [3, 4]. However, the popularity of FBP began to decline only a few years ago, when time-consuming IR became more feasible with the increase of computer speed and the development of the ordered subset method that improves the convergence rate of the ordered subset expectation maximization (OSEM) algorithm [5-8]. IR is now considered to be the state of the art and has been investigated in several phantom and patient studies [9-12]. In contrast, little is known about TrueX, an enhanced 3D iterative reconstruction, and its differences from the conventional 2D OSEM and 3D OSEM [13]. Recently, Knäusl et al. [14] published investigations with regard to PET-based volume segmentation on spherical objects with emphasis on the iterative TrueX algorithm, and concluded that TrueX must be used carefully for quantitative comparison. A similar conclusion was drawn earlier by a different group [15, 16]. Further investigations on the edge artifacts of TrueX were published by Tong et al. [17], in which a mitigation method using a post-reconstruction, band-suppression filter was proposed. Despite its usefulness, this approach is difficult to implement in clinical practice, since this kind of filter is not provided in the standard manufacturer's algorithms. TrueX is based on measured Point-Spread-Functions and models, correcting detector characteristics by taking into account lines of response (LOR) that originate from photons further away from the center of the field of view (FOV). The work of Panin et al. [18] provides a detailed technical description from the manufacturer's point of view.

Knäusl and co-workers also studied the partial volume effect (PVE). The PVE starts to make an impact in structures having a size in the order of the spatial resolution, leading to underestimates of the true activity concentration, as well an overestimation of small volumes. For correction purposes, one typically determines the recovery coefficients (RC), which are the ratios of the activity concentration displayed in the image over the measured true activity concentration. These RCs turn out to be stable for larger volumes, but decrease considerably for smaller ones due, to the PVE. RCs can refer to the maximum or mean activity concentration, depending on the evaluation method used.

DOI: 10.5963/LSMR0502001

Although "shell-less" lesions without an outer plastic shell have been developed [19, 20], the standard measurements performed for quality assurance in nuclear diagnostics still use phantoms with thin plastic walls [13]. It is well known that an inactive sphere wall contributes to the PVE [1, 21], but little data are available regarding to what extent, given that the majority of evaluation strategies rely on simple local or global thresholding. Despite its questionable scientific significance, tresholding is still a widespread method also used by Knausel et al. [14], and is even recommended by international experts' reports [22]. Nonetheless, thresholding performs poorly when detecting small objects [23], and thus has limitations. Furthermore, the use of spheres conceals the fact that the PVE occurs in objects of any shape as long as they have small spatial extensions in at least one dimension. Therefore, this work does not repeat the abovementioned phantom study with spheres, but focuses on non-spherical objects.

In summary, our study aims to deepen insights into the TrueX reconstruction algorithm by evaluating the following issues:

- The impact of different evaluation methods on image quantification.
- The contribution of inactive walls to the PVE.
- The effects that occur from measuring non-spherical objects.

For comparison, reconstruction and evaluation is performed analogously with 2-dimensional (2D) and 3-dimensional (3D) OSEM.

II. METHODS

Activity concentrations are given in [Bq/ml] and addressed as activity per volume (A/V) in all figures. Measurements on a Siemens Biograph 64 TruePoint™ PET/CT-Scanner were done using an in-house phantom (see Fig. 1).

Fig. 1 In-house constructed phantom with eight connected inner cylinders

The phantom consists of eight connected acrylic cylinders of different diameters, called in the inner phantom, surrounded by an acrylic cylinder, the so-called phantom body. Tables 1 and 2 list the parameters for this phantom. The slightly deviating inner length of the thickest cylinder stems from constraints in the manufacturing process and has no impact on the study.

TABLE 1 PHANTOM PARAMETERS OF THE INNER PHANTOM

inner diameter (mm)	inner length (mm)	wall thickness (mm)	Volume (ml)
4	59	2	0.7
11	59	2	5.6
16	59	2	11.9
24	59	3	26.7
34	59	3	53.6
44	59	3	89.7
64	59	3	189.8

DOI: 10.5963/LSMR0502001

84	51	3	282.6
Total:	464	-	660.6

TABLE 2 PHANTOM PARAMETERS OF THE PHANTOM'S BODY

inner diameter (cm)	inner length (cm)	wall thickness (cm)	Volume (ml)
18.8	74.5	0.5	12500

The reason for constructing our own phantom instead of using the well-known Jaszczak Phantom™, or the ACR phantom, both of which include cylindrical objects, is the considerably increased range of cylinder diameters. For the Deluxe Jaszczak Phantom™ and the ACR phantom, this range is 4.8 to 12.7 mm and 4.8 to 25 mm respectively, it is 4 to 84 mm in the newly constructed phantom.

For the measurements, the phantom was filled with 18F-FDG, producing A/Vs with signal to background ratios (SBR) of 2:1, 4:1, 6:1, and 8:1. As shown in Table 3, this corresponds to an average A/V for the entire phantom of between 5 and 10 kBq/ml, thus fulfilling the quality assurance conditions in Nuclear Medicine when measuring a standard NEMA phantom [24, 25].

TABLE 3 DIFFERENT RATIOS FOR ACTIVITY CONCENTRATION

foreground A/V [kBq/ml]	background A/V [kBq/ml]	ratio	total A/V [kBq/ml]
17	8.3	2:1	8.7
26	6.5	4:1	7.4
30	4.9	6:1	6.2
32	3.9	8:1	5.3

As mentioned in the introduction, three different iterative reconstruction methods were taken into account: TrueX (4 iterations, 21 subsets), OSEM 2D (4 iterations, 8 subsets), and OSEM 3D (4 iterations, 8 subsets). Since the aim of this study is to investigate issues relating to clinical practice, the number of iterations and subsets correspond to standard clinical protocol. All reconstruction algorithms were applied using a Gaussian filter on the one hand and omitting all kinds of filters on the other, also called allpass mode. The Gaussian filter was a post-reconstruction filter with a constant kernel size of $5 \times 5 \times 5$.

For post processing, the PET data were analyzed with in-house codes written on IDL (EXELIS), which were validated in another study [23]. The phantom was placed in the scanner so that the cylinder axis was identical to the z-axis. Initial regions of Interest (ROI) around each inner cylinder were drawn by hand [23]. Three different procedures were used to determine the mean activity concentration in each cylinder, denoted here as Adaptive Thresholding, Percentage Thresholding, and the Maximum Line Method. The voxel size was always $4.1 \times 4.1 \times 4{,}1\ mm^3$.

The Adaptive Thresholding algorithm is applied to each individual ROI and works as follows: it starts with a small initial threshold with regard to the A/V and calculates the resulting volume produced by the voxels with values exceeding the initial threshold. The thereby segmented volume is compared to the known true cylinder volume and adapted by increasing the cutoff value, the threshold. This step is repeated until the difference between the segmented and true volumes reaches a minimum. Segmented volumes have to form a three-dimensional connected volume in order to be considered a meaningful segmentation result. Naturally, the above algorithm also includes voxels from the inactive acrylic walls. Thus, following Adaptive Thresholding, the outer hulls are subtracted by employing shrinking operations on the basis of a first-order neighborhood. Several cylindrical layers of voxels, called hulls hereafter, were successively subtracted, evaluating the effect on segmentation.

With regard to Percentage Thresholding, a threshold is applied, representing the percentages (36 % and 42 %) [26-28] of the global maximum voxel value present in the entire image. As in Adaptive Thresholding, the outer hulls were subtracted in order to cut the voxels that were comprising parts of the inactive plastic walls. Once again, segmentation results that are not morphologically connected are not considered meaningful.

Finally, the so called Maximum Line Method is introduced. For each ROI, the algorithm locates the voxel with the maximum intensity and considers all voxels situated in the line parallel to the cylinder axis. The reason for its introduction can be found in the in the wide-spread recommendation that for small volumes, the maximum activity best represents the true activity for commonly used reconstruction [14, 29]. The Maximum Line Method is an extension of this recommendation, can be easily implemented into standard image processing software like ImageJ, and has slightly better statistical significance than the voxel with the maximum activity alone.

III. RESULTS

DOI: 10.5963/LSMR0502001

The A/V evaluated from the reconstructed PET images is given the as ratio over the true A/V. Since no differences were observed between the results from Gaussian filtering and those from the allpass mode, only the results for the latter are presented. Moreover, only the results that satisfy the aforementioned criterion of a meaningful segmentation result, i.e. a three dimensional connected volume, are displayed.

Fig. 2 shows the effect on the evaluated A/V and its respective standard deviation when the hulls are gradually stripped off after applying Adaptive Thresholding.

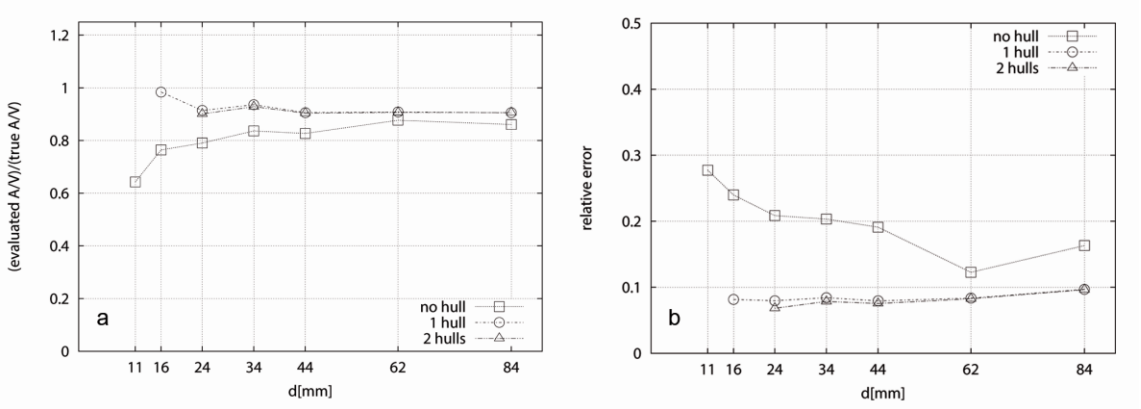

Fig. 2 Effect on the evaluated A/V when hulls are gradually stripped off after applying Adaptive Thresholding. a: Ratio of evaluated over true A/V of the inner phantom (SBR: 8:1) as function of the cylinders' diameter with and without the reduction of up to four shells by using Adaptive Thresholding of an OSEM 3D reconstructed image. b: Corresponding relative uncertainty

Without the subtraction of any layers, the results resemble the well-known pattern of PET phantom measurements using filled plastic objects, a general underestimate (~15%) of the A/V for larger objects that increases with decreasing diameter of the segmented object and reaches 35% for the cylinder with a diameter of 11 mm. However, stripping off the first hull not only reduces the general underestimation to 5 - 10%, but also compensates for the PVE that originates from the inactive plastic walls. This results in reconstructed A/Vs that are almost constant over the entire range of diameters. This is also mirrored in the behavior of the relative uncertainty of the evaluated A/V, considerably higher in the case where no hull is subtracted and increases with smaller diameters where the fraction of voxels containing parts of the wall is higher. Likewise, subtracting the hulls results in an almost diameter–independent relative uncertainty of about 0.1. Stripping off more than one hull results in a failed detection of the cylinders with diameters less than 16 mm as shown in Fig. 2. This is why, hereafter, all further segmentation results with regard to Adaptive Thresholding, as well as Percentage Thresholding, refer to the subtraction of only the first hull. The effects described above are observed with regard to all reconstruction algorithms.

Fig. 3 shows the results of Adaptive Thresholding for the TrueX as well as the OSEM 2D and OSEM 3D.

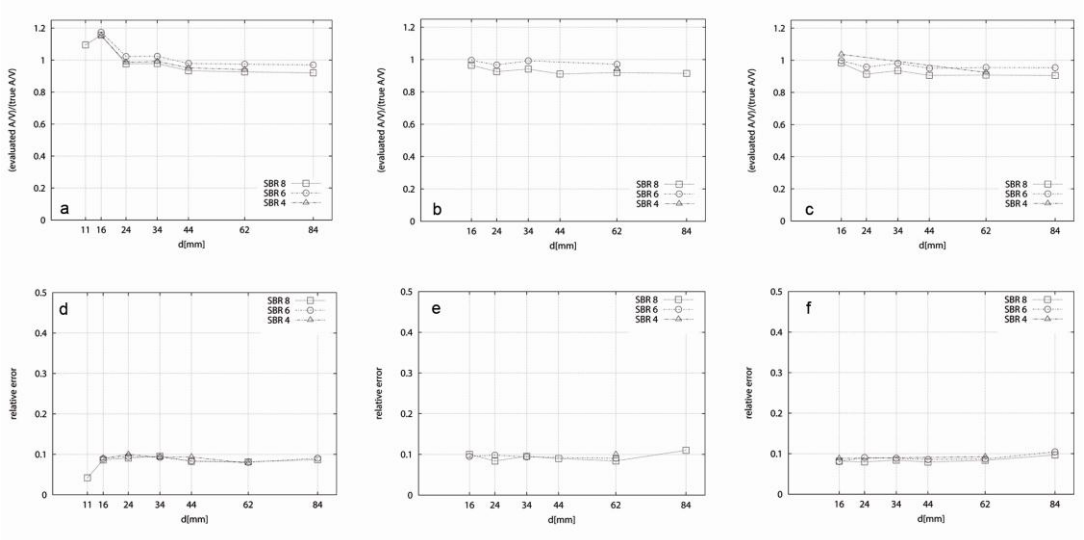

Fig. 3 Ratio of evaluated over true A/V of the inner phantom with different SBRs. Evaluated with Adaptive Thresholding of a TrueX (a), OSEM 2D (b), OSEM 3D (c) and reconstructed image with 1 subtracted outer hull. Corresponding relative uncertainty of TrueX (d), OSEM 2D (e) and OSEM 3D (f)

While, Figs. 3b and 3c superbly reproduce the true activity concentration with a deviation of only 5%, TrueX shows an overestimation of up to 25% in an area between diameters of 11 mm and 24 mm (see graphic a in Fig. 3). The standard deviation with regard to the segmented area stays constant (approximately 10 %) for all reconstruction algorithms. It is

DOI: 10.5963/LSMR0502001

important to note the fact that for a given SBR, not all cylinders are detected with Adaptive Thresholding. One can say that the probability of detection decreases with cylinder diameter and SBR. The 4 mm cylinder, as well as all cylinders at SBR 2:1, were never detected. Tables 4 to 6 summarize the detection capacity for different SBRs, evaluation strategies, and reconstruction algorithms.

TABLE 4 NUMBERS OF DETECTED CYLINDERS AS A FUNCTION OF THE SBR, THE EVALUATION STRATEGY OF THE RECONSTRUCTION ALGORITHM OSEM 2D

Evaluation strategy	**8:1**	**6:1**	**4:1**	**2:1**
Adaptive Thresholding	6	4	0	0
Percentage Thresholding 36 %	8	7	5	0
Percentage Thresholding 42 %	7	7	7	0
Maximum Line Method	8	8	8	8

TABLE 5 NUMBERS OF DETECTED CYLINDERS AS A FUNCTION OF THE SBR, THE EVALUATION STRATEGY OF THE RECONSTRUCTION ALGORITHM OSEM 3D

Evaluation strategy	**8:1**	**6:1**	**4:1**	**2:1**
Adaptive Thresholding	6	6	2	0
Percentage Thresholding 36 %	7	7	6	0
Percentage Thresholding 42 %	7	7	8	0
Maximum Line Method	8	8	8	8

TABLE 6 NUMBERS OF DETECTED CYLINDERS AS A FUNCTION OF THE SBR, THE EVALUATION STRATEGY OF THE RECONSTRUCTION ALGORITHM TRUEX

Evaluation strategy	**8:1**	**6:1**	**4:1**	**2:1**
Adaptive Thresholding	7	6	5	0
Percentage Thresholding 36 %	7	7	7	0
Percentage Thresholding 42 %	7	7	7	0
Maximum Line Method	8	8	8	8

In Fig. 4 and Fig. 5, the results of Percentage Thresholding with 36 % and 42 %, respectively, are displayed.

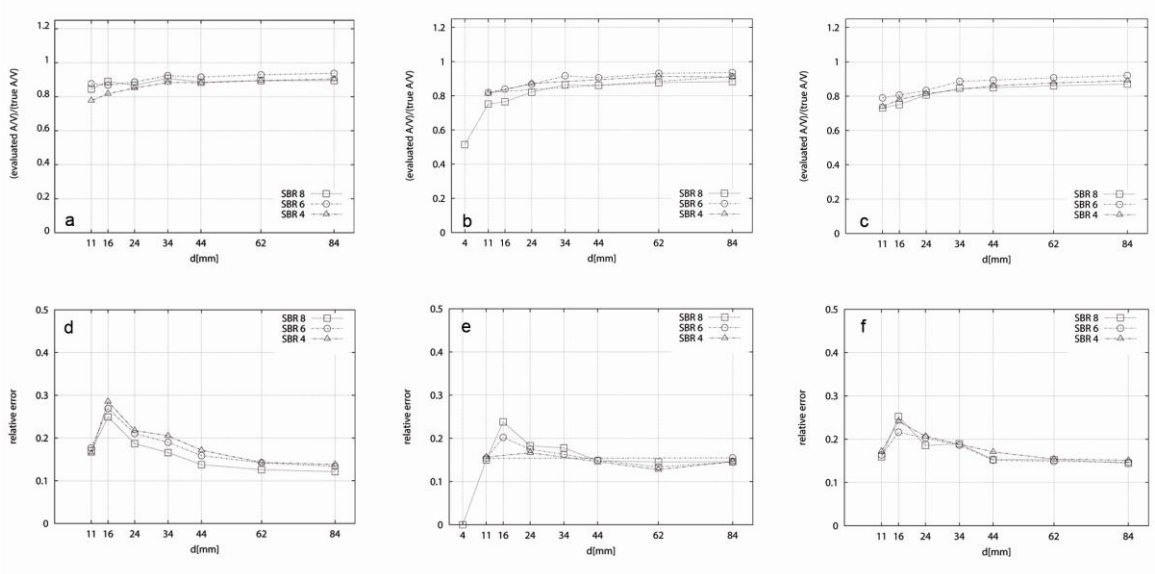

Fig. 4 Ratio of evaluated over true A/V of the inner phantom with different SBRs. Evaluated with 36 % Thresholding of a TrueX (a), OSEM 2D (b), OSEM 3D (c) and reconstructed image with 1 subtracted outer hull. Corresponding relative uncertainty of TrueX (d), OSEM 2D (e) and OSEM 3D (f)

DOI: 10.5963/LSMR0502001

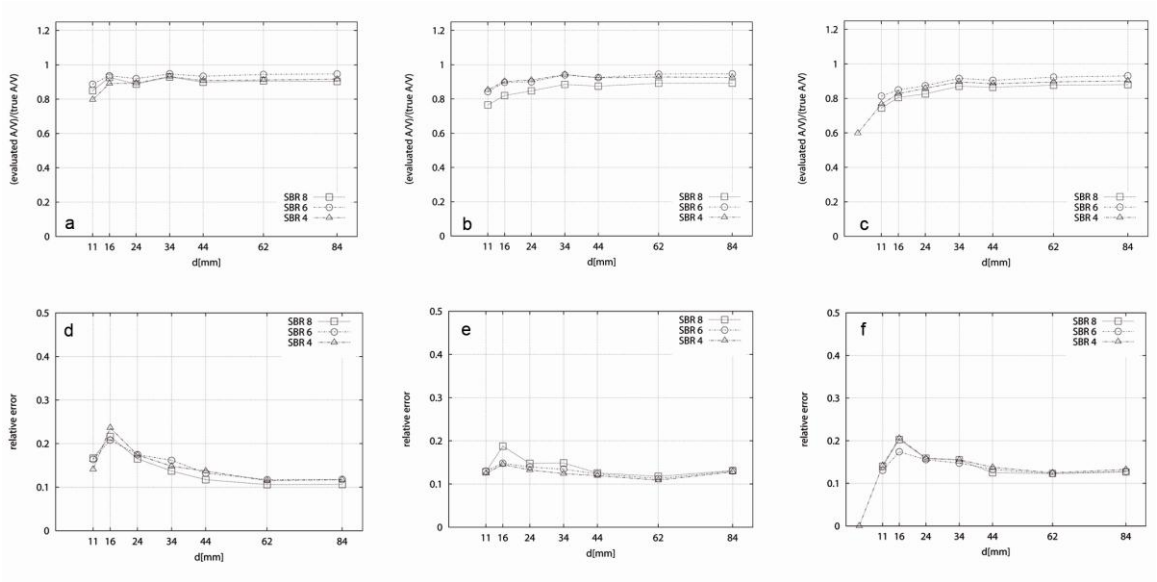

Fig. 5 Ratio of evaluated over true A/V of the inner phantom with different SBRs. Evaluated with 42 % Thresholding of a TrueX (a), OSEM 2D (b), OSEM 3D (c) and reconstructed image with 1 subtracted outer hull. Corresponding relative uncertainty of TrueX (d), OSEM 2D (e) and OSEM 3D (f)

42 % Thresholding underestimates the activity concentration with regard to OSEM 2D and OSEM 3D for cylinders with a diameter larger than 34 mm by ~10%. For smaller diameters, the underestimation increases. A similar behavior can be seen with TrueX, where a constant underestimate of about 10% is observed down to the diameter of 16 mm. For cylinders smaller than 16 mm, the underestimate again increases. The relative uncertainties for this evaluation method increase with decreasing diameter, reaching their maximum at 16 mm with 25% for the 42% threshold and 30% for the 36% threshold. Below this value, the standard deviation decreases due to the small number of voxels. Percentage Thresholding clearly detects more cylinders than Adaptive Thresholding, and for some combinations (see Fig. 4b, 36 % Thresholding of OSEM 2D and a SBR of 8:1), even the cylinder with a diameter of 4 mm is detected. Nonetheless, at SBR 2:1, the segmentation yield is zero.

Fig. 6 depicts the results of the third evaluation strategy, the Maximum Line method.

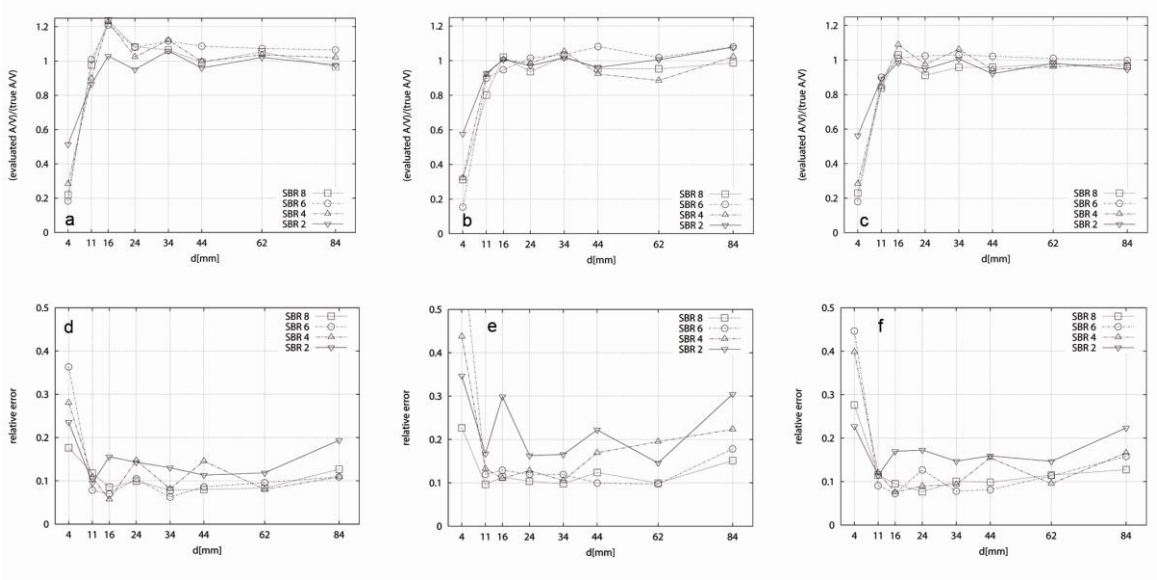

Fig. 6 Ratio of evaluated over true A/V of the inner phantom with different SBRs. Evaluated with maximum line method of a TrueX (a), OSEM 2D (b), OSEM 3D (c). Corresponding relative uncertainty of TrueX (d), OSEM 2D (e) and OSEM 3D (f)

Due to the nature of the maximum line method, all cylinders of all SBRs are detected, whereas the lower number of considered voxels results in worse statistics, and consequently, a higher relative uncertainty with larger fluctuations. TrueX shows the same behavior as Adaptive Thresholding with an outlier for diameters between 11 mm and 24 mm, where the A/V is overestimated up to 25% for SBRs of 4:1 and higher. For diameters of 16 mm and larger, 2D OSEM and 3D OSEM yield a deviation of the A/V of approximately 10%. However, in contrast to the previous evaluation methods, not only underestimates are observed but rather divergences in both directions, likely as a result of the lower statistics. However, for diameters below 16 mm, again, an increasing underestimation is evident.

DOI: 10.5963/LSMR0502001

In summary, 3D OSEM yields the best results in terms of A/V reconstruction with regard to all evaluation strategies.

IV. DISCUSSION

The goal of this study was to investigate the impact of Iterative Reconstruction algorithms emphasizing the TrueX algorithm and the evaluation strategy on the outcome of quantitative phantom studies using non-spherical objects. The study included the reconstruction algorithms TrueX, 2D-OSEM, and 3D-OSEM, and made use of three different techniques of data evaluation, Adaptive Thresholding, Percentage Thresholding, and the Maximum Line Method.

As for the main objective of this study, the investigation of the TrueX algorithm, the conclusions of Knäusl et al. [14] Mollina-Duran [15], and Tong et al. [17] are confirmed. TrueX produces edge artifacts and therefore, rather large uncertainties, when it comes to quantitative studies. According to Mollina-Duran [15], this can also be related to the conversion of the algorithm. This is demonstrated by TrueX's overestimate of the A/V of up to 25% at diameters between 11 mm and 24 mm in contrast to the much smaller deviations produced by 2D OSEM and 3D OSEM. As shown by Tong et al. [17] for spheres with a diameter ≥ 6.5 mm, TrueX very accurately reproduces the activity concentration in the absence of background activity while yielding an overestimation when background activity is added. This raises the question of whether the Point-Spread-Functions incorporated in TrueX were measured under practical conditions, such as applying different SBRs.

In clinical practice, the visual interpretation of lesions is still more common than quantification. However, when the Standard Uptake Value (SUV) is calculated, very often the highest pixel value of such a visually detected lesion is used for calculation. Consequently, TrueX might enable a better visual detection of otherwise missed tumors. Nonetheless, for quantitative analysis, 2D OSEM or 3D OSEM are the better choice due to more accurate SUVs. The post-reconstruction, band-suppression filter suggested by Tong et al. [17] improves the quantitative results for TrueX in phantoms, but not so much in the clinical routine. Furthermore, the technique of stripping the outer hull of voxels when using Adaptive and Percentage Thresholding considerably reduces the contribution of the PVE stemming from the inactive walls. This results in reduced underestimates of the activity concentration, as well as a reduced relative uncertainty. Both phenomena prove to be insensitive to the objects' diameter. Therefore, introducing the technique of hull-stripping for standard phantom measurements could change the way activity analysis is performed. The large variety of exponential regression curves in previous research [14, 30] could be replaced by a correction factor, which is almost constant over the entire range of diameters (see Fig. 2), and thus considerably facilitates activity analysis. As shown in Fig. 3, the cylinders detected by Adaptive Thresholding plus hull-stripping (diameters ≥ 16mm) are virtually devoid of PVE, whereas Percentage Thresholding plus hull- stripping still underestimates the value of the A/V to a certain extent, as seen in Figs. 4 and 5. Thus, this underlines the advantage of Adaptive Thresholding with hull-stripping. Finally, when using the Maximum Line Method, this study is in accordance with Knäusl et al. (2012) in that it demonstrates that for diameters smaller than 16 mm, the PVE increases exponentially, as displayed in Fig. 6.

Another interesting insight comes from closely investigating the statement found in the literature that for the OSEM algorithm, the maximum activity in a specific volume yields the true activity when using a SBR independent correction factor C that depends on the sphere size. For spheres larger than 2.5 ml (i.e. with a diameter larger than 17 mm), C is given there as 1.1 [14]. After stripping the outside shell, Adaptive Thresholding underestimates the activity concentration by ~5% and Percentage Thresholding underestimates it by ~10%. Thus, applying C to the results of this work would perfectly correct Percentage Thresholding and yield a slight overestimate for Adaptive Thresholding. However, at this point, it is important to note that the correction factor for the maximum activity was determined in a specific volume, whereas both thresholding methods applied here produce a mean value. Applying C to the results from the Maximum Line Method would result in an overestimate for many given diameters and SBRs. Moreover, applying C to the maximum value itself could even worsen this overestimate, since the Maximum Line Method represents the mean voxel value of the row parallel to the cylinder axis containing the voxel with maximum intensity. Therefore, it can be concluded that the correction factor C has limitations in application.

The maximum foreground volume used by Knaeusl et al. [14] is 11.5 ml, corresponding to the third smallest foreground volume of this work. Larger volumes, however, represent a larger statistical ensemble, and thus a higher probability of single outliers from the statistical mean. In our case, such an outlier corresponds to the maximum value of the activity concentration. As a consequence, the recommendation of using the maximum activity in a specific volume as an estimate for the true activity with regard to OSEM must be strictly limited to measurements with identical or similar parameters as chosen by Knaeusl et al. [14]. On the other hand, larger and non-spherical volumes require a more detailed analysis like the evaluation strategies presented here. Furthermore, this study cannot confirm the correction factors' independence with regard to the SBR.

When comparing the different evaluation strategies, one clearly sees that with regard to unfavorable circumstances like small diameters (≤ 11mm) and small SBRs like 2:1, only the Maximum Line Method guarantees the detection of all cylindrical objects. The main reason for this is that the restriction on morphologically connected segmentation results dismisses solutions despite quantitatively good agreement. One could argue that in clinical settings, tumors and metastases often appear disseminated. However, a phantom study like this is about pattern recognition, and therefore, the aim should be the exact reconstruction of the measured pattern. The smallest uncertainty, however, is attributed to Adaptive Thresholding (~5%). On

DOI: 10.5963/LSMR0502001

the other hand, the disadvantage of the Maximum Line Method is its very limited statistical significance.

Using a phantom that contains cylinders instead of spheres casts a different light on activity analysis. Whereas for spheres, the two parameters "volume" and "diameter" ultimately stand for the same dependence, namely the size, they get decoupled when using cylindrical objects. The diameter has a strong influence on the magnitude of the PVE. In turn, large volumes make the technique of using the maximum activity concentration as an estimate for the true activity not advisable. In the future, it would be meaningful to extend this project with phantoms containing objects of other shapes.

V. CONCLUSION

For quantitative studies, such as quality assurance measurements with standard phantoms, OSEM 3D should be preferred.

Stripping the outer hull of voxels when using Adaptive and Percentage Thresholding considerably reduces the contribution of the PVE stemming from inactive plastic walls. Such procedures should become part of segmentation strategies, given that among other things, they enable a PVE correction with a factor that is more constant over the entire range of diameters. Adaptive Thresholding with hull-stripping quasi-nullifies the PVE for diameters >16 mm.

In the case that an object is not detected by Adaptive Thresholding, the Maximum Line Method is a reliable alternative with only small deviations for diameters >16 mm.

The recommendation of using the maximum activity in a specific volume as an estimate for the true activity must be handled with care when applied to TrueX reconstructions, as seen in Fig. 6b.

In accordance with previous work, caution is recommended when applying TrueX reconstruction.

REFERENCES

[1] W. A. Weber and R. Figlin, "Monitoring cancer treatment with PET/CT: does it make a difference?" *Journal of nuclear medicine*, vol. 48(Suppl 1), pp. 36-44, 2007.

[2] B. F. Hutton, "An introduction to iterative reconstruction," *Rev med nucl Alasbimn J*, vol. 5(18), 2002.

[3] L. A. Shepp and Y. Vardi, "Maximum likelihood reconstruction for emission tomography," *IEEE transactions on medical imaging*, vol. 1(2), pp. 113-22, 1982.

[4] K. Lange and R. Carson, "EM reconstruction algorithms for emission and transmission tomography," *Journal of computer assisted tomography*, vol. 8(2), pp. 306-16, 1984.

[5] H. M. Hudson and R. S. Larkin, "Accelerated image reconstruction using ordered subsets of projection data," *IEEE transactions on medical imaging*, vol. 13(4), pp. 601-9, 1994.

[6] C. X. Wang, W. E. Snyder, G. Bilbro, and P. Santago, "Performance evaluation of filtered backprojection reconstruction and iterative reconstruction methods for PET images," *Computers in biology and medicine*, vol. 28(1), pp. 13-24, 1998.

[7] R. E. Carson, Y. Yan, B. Chodowsky, T.K. Yap, and M. E. Daube-Witherspoon, "Precision and accuracy of regional radioactivity quantitation using the maximum likelihood EM reconstruction algorithm," *IEEE transactions on medical imaging*, vol. 13(3), pp. 526-37, 1994.

[8] C. T. Mesina, R. Boellaard, G. Jongbloed, A. W. van der Vaart, and A. A. Lammerstsma, "Experimental evaluation of iterative reconstruction versus filtered back projection for 3D [15O]water PET activation studies using statistical parametric mapping analysis," *NeuroImage*, vol. 19(3), pp. 1170-9, 2003.

[9] R. Boellaard, A. Van Lingen, and A. A. Lammertsma, "Experimental and clinical evaluation of iterative reconstruction (OSEM) in dynamic PET: quantitative characteristics and effects on kinetic modeling," *Journal of nuclear medicine: official publication, Society of Nuclear Medicine*, vol. 42(5), pp. 808-17, 2001.

[10] C. Riddell, R. E. Carson, J. A. Carrasquillo, S. K. Libutti, D. N. Danforth, M. Whatley, et al., "Noise reduction in oncology FDG PET images by iterative reconstruction: a quantitative assessment," *Journal of nuclear medicine*, vol. 42(9), pp. 1316-23, 2001.

[11] M. Lubberink, R. Boellaard, A. P. van der Weerdt, F. C. Visser, and A. A. Lammertsma, "Quantitative comparison of analytic and iterative reconstruction methods in 2- and 3-dimensional dynamic cardiac 18F-FDG PET," *Journal of nuclear medicine*, vol. 45(12), pp. 2008-15, 2004.

[12] M. Krzywinski, V. Sossi, and T. J. Ruth, "Comparison of FORE, OSEM and SAGE algorithms to 3DRP in 3D PET using phantom and human subject data," *IEEE Transactions on Nuclear Science*, vol. 46(4), pp. 1114-1120, 1999.

[13] J. Ironside, S. Leonard, N. McDonald, and S. Spies, "A phantom study to evaluate variations in the quantization derived from a new 3D reconstruction algorithm," *Society of Nuclear Medicine, Annual Meeting Abstracts*, vol. 50(2), pp. 2242, 2009.

[14] B. Knaeusl, A. Hirtl, G. Dobrozemsky, H. Bergmann, K. Kletter, R. Dudczak, et al., "PET based volume segmentation with emphasis on the iterative TrueX algorithm," *Zeitschrift für medizinische Physik*, vol. 22(1), pp. 29-39, 2012.

[15] F. Molina-Duran, D. Dinter, F. Schoenahl, S. O. Schoenberg, and G. Glatting, "Dependence of image quality on acquisition time for the PET/CT Biograph mCT," *Z Med Phys*, vol. 24, pp. 73-9, 2014.

[16] D. M. Dommett, N. Keat, and W. A. Hallett, "Evaluation of the Siemens TrueX reconstruction algorithm for quantitative PET studies," *World Molecular Imaging Congress*, Montréal, Canada, pp. 23-26, 2009.

[17] S Tong, A. M. Alessio, K. Thielemanns, C. Stearns, S. Ross, and P. E. Kinahan, "Properties and Mitigation of Edge Artifacts in PSF-Based PET Reconstruction," *IEEE Transactions on Nuclear Science*, vol. 58(5), pp. 2264-2275, 2011.

DOI: 10.5963/LSMR0502001

[18] V. Y. Panin, F. Kehren, C. Michael, and M. Casey, "Fully 3-D PET reconstruction with system matrix derived from point source measurements," *IEEE transactions on medical imaging*, vol. 25(7), pp. 907-21, 2006.

[19] D. J. Kadrmas, M. E. Casey, N. F. Black, J. J. Hamill, V. Y. Panin, and M. Conti, "Experimental Comparison of Lesion Detectability for Four Fully-3D PET Reconstruction Schemes," *IEEE Trans Med Im*, vol. 28(4), pp. 523-534, 2009.

[20] D. J. Kadrmas, M. E. Casey, M. Conti, B. W. Jakoby, C. Lois, and D. W. Townsend, "Impact of Time-of-Flight on PET Tumor Detection," *J Nucl Med*, vol. 50, pp. 1315-1323, 2009.

[21] B. Berthon, C. Marshall, A. Edwards, M. Evans, and E. Spezi, "Influence of cold walls on PET image quantification and volume segmentation: a phantom study," *Med. Phys.*, vol. 40, pp. 082505, 2013.

[22] M. MacManus, U. Nestle, K. E. Rosenzweig, I. Carrio, C. Messa, O. Belohlavek, et al., "Use of PET and PET/CT for radiation therapy planning," *IAEA expert report 2006-2007, Journal of the European Society for Therapeutic Radiology and Oncology*, vol. 91(1), pp. 85-94, 2009.

[23] T. Layer, M. Blaickner, B. Knäusl, D. Georg, J. Neuwirth, R. P. Baum, R., et al., "PET image segmentation using a Gaussian mixture model and Markov random fields," *EJNMMI Physics*, vol. 2 (9), 2015.

[24] H. Herzog, L. Tellmann, C. Hocke, U. Pietrzyk, M. E. Casey, and T. Kuwert, "NEMA NU2-2001 guided performance evaluation of four Siemens ECAT PET scanners," *IEEE Transactions on Nuclear Science*, vol. 51(5), pp. 2662-2669, 2004.

[25] B W Jakoby, Y Bercier, M Conti, M E Casey, B Bendriem, and D W Townsend, "Physical and clinical performance of the mCT time-of-flight PET/CT scanner," *Phys. Med. Biol.*, vol. 56, p. 2375, 2011.

[26] H. Vees, S. Senthamizhchelvan, R. Miralbell, D. C. Weber, O. Ratib, and H. Zaidi, "Assessment of various strategies for 18F-FET PET-guided delineation of target volumes in high-grade glioma patients," *EJNMMI*, vol. 36(2), pp. 182-93, 2009.

[27] Y. E. Erdi, K. Rosenzweig, A. K. Erdi, H. A. Macapinlac, Y. Hu, L. E. Braban, et al., "Radiotherapy treatment planning for patients with non-small cell lung cancer using positron emission tomography (PET)," *Journal of the European Society for Therapeutic Radiology and Oncology*, vol. 62(1), pp. 51-60, 2002.

[28] Y. E. Erdi, O. Mawlawi, S. M. Larson, M. Imbriaco, H. Yeung, R. Finn R, et al., "Segmentation of lung lesion volume by adaptive positron emission tomography image thresholding," *Cancer*, vol. 80(12), pp. 2505-9, 1997.

[29] M. Bazañez-Borgert, R. A. Bundschuh, M. Herz, M. J. Martinez, M. Schwaiger, and S. I. Ziegler, "Radioactive spheres without inactive wall for lesion simulation in PET," *Zeitschrift für medizinische Physik*, vol. 18(1), pp. 37-42, 2008.

[30] M. Brambilla, R. Matheoud, C. Secco, G. Loi, M. Krengli, and E. Inglese, "Threshold segmentation for PET target volume delineation in radiation treatment planning: the role of target-to-background ratio and target size," *Medical physics*, vol. 35(4), pp. 1207-13, 2008.

DOI: 10.5963/LSMR0502001